ELSEVIER

Clinical Research, Basic Science

Stress Analysis in AAA does not Predict Rupture Location Correctly in Patients with Intraluminal Thrombus

Fanny Lorandon, MD,[1] Simon Rinckenbach, MD, PhD,[1,2] Nicla Settembre, MD, PhD,[3] Eric Steinmetz, MD, PhD,[4] Lucie Salomon Du Mont, MD, PhD,[1,2] and Stephane Avril, PhD,[5] Saint Etienne France

Abstract: Background: A biomechanical approach to the rupture risk of an abdominal aortic aneurysm could be a solution to ensure a personalized estimate of this risk. It is still difficult to know in what conditions, the assumptions made by biomechanics, are valid. The objective of this work was to determine the individual biomechanical rupture threshold and to assess the correlation between their rupture sites and the locations of their maximum stress comparing two computed tomography scan (CT) before and at time of rupture.

Methods: We included 5 patients who had undergone two CT; one within the last 6 months period before rupture and a second CT scan just before the surgical procedure for the rupture. All DICOM data, both pre- and rupture, were processed following the same following steps: generation of a 3D geometry of the abdominal aortic aneurysm, meshing and computational stress analysis using the finite element method. We used two different modelling scenarios to study the distribution of the stresses, a “wall” model without intraluminal thrombus (ILT) and a “thrombus” model with ILT.

Results: The average time between the pre-rupture and rupture CT scans was 44 days (22–97). The median of the maximum stresses applied to the wall between the pre-rupture and rupture states were 0.817 MPa (0.555–1.295) and 1.160 MPa (0.633–1.625) for the "wall" model; and 0.365 MPa (0.291–0.753) and 0.390 MPa (0.343–0.819) for the "thrombus" model. There was an agreement between the site of rupture and the location of maximum stress for only 1 patient, who was the only patient without ILT.

Conclusions: We observed a large variability of stress values at rupture sites between patients. The rupture threshold strongly varied between individuals depending on the intraluminal thrombus. The site of rupture did not correlate with the maximum stress except for 1 patient.

INTRODUCTION

The challenge in managing patients with aortic aneurysms is to estimate the relationship between the surgical risk and the benefit of no rupture. Actually, defining the rupture risk of an asymptomatic or symptomatic abdominal aortic aneurysm (AAA) is essential for patients with this condition. By consensus, a maximum aneurysm diameter of 55 mm represents the current surgical indication for AAA.[1–3] However, this diameter threshold does not consider inter-individual variability. Indeed, small aneurysms may also

Conflict of interest: The authors have no conflicts of interest to disclose.

[1]*Department of Vascular and Endovascular Surgery, University Hospital of Besançon, Besançon, Saint Etienne, France.*
[2]*EA3920, University Hospital of Besançon, Besançon, France.*
[3]*Department of Vascular Surgery, University Hospital of Nancy, Nancy, France.*
[4]*Department of Vascular Surgery, University Hospital of Dijon, Dijon, France.*
[5]*Mines Saint-Etienne, Univ Lyon, INSERM, U 1059 Sainbiose, Centre CIS, F - 42023 Saint-Etienne, France.*

Correspondence to: Fanny Lorandon, MD, Department of Vascular Surgery, Centre Hospitalier Regional de Besancon, Boulevard Alexandre Fleming, 25000 Besançon, France.; E-mail: lorandon.fanny@hotmail.fr or avril@emse.fr

Ann Vasc Surg 2021; 000: 1–11
https://doi.org/10.1016/j.avsg.2021.08.008

Manuscript received: December 20, 2020; manuscript revised: August 21, 2021; manuscript accepted: August 31, 2021; published online: xxx

be prone to rupture, while very large aneurysms may be observed without any symptoms.[1,4]

Numerical simulation using Finite Element Analyses (FEA) is an approach that could enable the prediction of rupture risks. Rupture of an aneurysm occurs when the local wall stress exceeds the local wall strength. Mechanical stresses mostly depend on the luminal pressure and on the arterial geometry, whereas the wall strength is a patient-specific material property. The latter being unknown, research focused on stress estimation. Several studies highlighted the relevance of biomechanical markers to estimate a risk of rupture by integrating factors such as patient geometry and characteristics into biomechanical criteria.[5–10] However, although they are statistically relevant, the significance of biomechanical markers at the individual level remains to be demonstrated.

Moreover, the mechanisms leading to ruptures are not yet completely understood. Identifying the mechanism of rupture would enable to define more precisely an individual risk of rupture. A biomechanical approach to the rupture risk of an abdominal aortic aneurysm (AAA) could be a solution to ensure a personalized estimate of this risk. It is still difficult to know in what conditions, the assumptions made by biomechanics, are valid.

The objective of this work was to determine the individual biomechanical rupture threshold and to assess the correlation between their rupture sites and the locations of their maximum stress comparing two Computed tomography (CT) scan before and at time of rupture.

MATERIALS AND METHODS

We have conducted a retrospective study. The FEA method was applied to perform stress analyses on 5 patients who had a CT scan at the time of rupture and a CT scan within the 6 months prior to rupture. The use of these scan datasets permitted studying the evolution of the stresses of an AAA in the 6 months preceding the rupture.

Study Population

Between 2010 and 2017, all patients who were managed urgently in the Vascular Surgery Department of Nancy, Dijon or Besancon for ruptured AAA were studied. Only patients treated for ruptured abdominal aortic aneurysm with CT scan diagnosis were taken into account. They also had to have an abdominal CT scan done in the 6 months before rupture to be included. CT scans of ruptured AAA revealed an extravasation of contrast material associated with an intra- or retroperitoneal hematoma. Any patient with a posterior aneurysmal rupture or associated with infectious or inflammatory aorta was excluded. We decided to study only patients with a case of anterior or lateral rupture. Chronic posterior ruptures are partly related to friction with vertebral bodies and are therefore part of a different biomechanical failure mechanism.[11] We chose to exclude posterior aneurysm rupture as, according to current theory, the spine plays a critical role in the posterial rupture[12,13] but it was not incorporated in our model. The failure sites were then identified, when it was possible to visualize a contrast extravasation.[14]

Computational Modelling

The same protocol was applied for all models: generation of a 3D geometry of the lumen and thrombus of the AAA, volume meshing, and calculation of biomechanical criteria (Fig. 1). We chose to study a model without thrombus and a model with thrombus. The aneurysmal wall was modelled with shell elements[15] whereas the thrombus was modelled with solid elements. FEA were performed by a single investigator.

Segmentation

Simpleware™ ScanIP (Version N-2018.03-SP1; Synopsys, Inc., Mountain View, USA) was used to process CT DICOM datasets. The data were segmented in a semi-automatic way, based on thresholding criteria. For each CT scan, we segmented the lumen and thrombus of the AAA between the renal arteries and the aortic bifurcation. The segmentation of ruptured AAAs excluded the extra peritoneal hematoma which was identified thanks to the lower concentration of contrast agent after the haemorrhagic shock. The smoothing factor for all cases was assumed to be the same.

Mesh

The Synopsys' Simpleware™ FE module was used for volumetric mesh generation. Each 3D geometry was meshed using quadratic tetrahedral 3D elements. A previous mesh size study permitted to determine the optimal mesh size, with about 150,000 nodes and 160,000 elements for each FEA.

Finite Element Analysis

FEA were conducted using the Abaqus/CAE 2018 software (Dassault Systemes, SIMULIA, RI, USA).

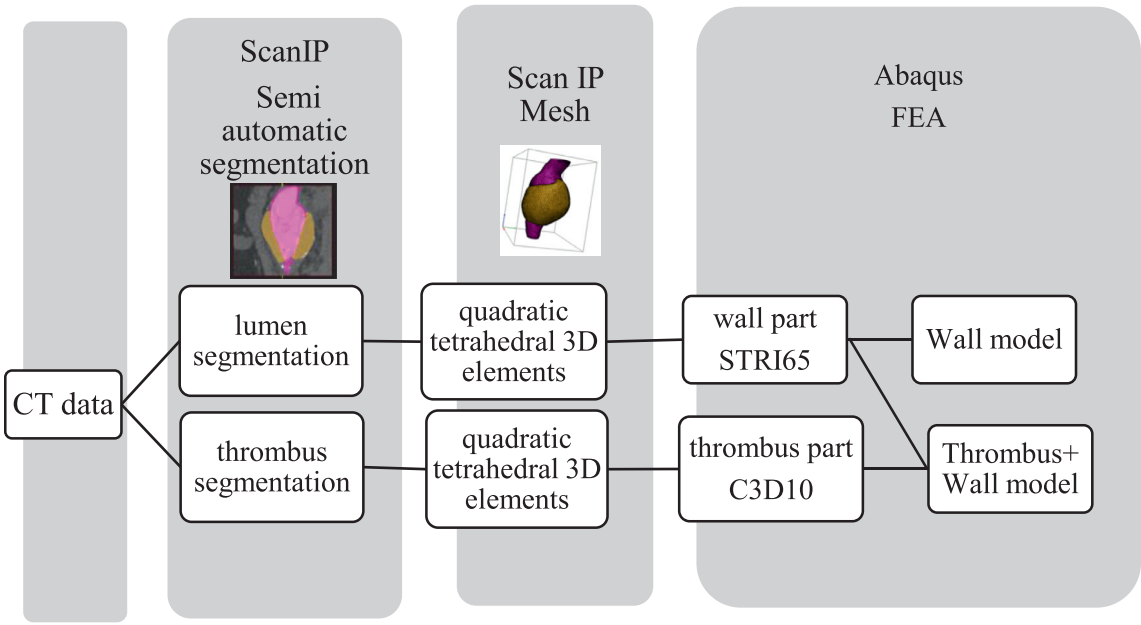

Fig. 1. Steps of Finite Element Analyses.

We used two different modelling scenarios to study stress distributions. In the first scenario, the model consisted of a wall part, the pressure being applied onto it. In the second scenario, the model consisted of a wall part and a thrombus part. The pressure was applied on the inner surface.

To create the wall part from Abaqus, a membrane composed of STRI65 elements was applied to the entire aneurysm to reproduce the aortic wall, defined with a thickness of 1.5 mm.[8]

The thrombus part consisted of C3D10 elements. It was assumed to be completely tied to the wall part by merging the common nodes of the boundary.

Such analysis on AAA usually requires computing the zero-pressure geometry of the aorta. Since such computation can only be achieved when the patient-specific material properties are known, we preferred using the assumption proposed by Joldes et al. They performed the stress analysis using linear elastic behaviour and infinitesimal strains, ratio between wall stiffness and thrombus stiffness should be about 20:1. The wall part was assigned a Young's modulus of 100,000 MPa, and a Poisson's ratio of 0.48. The thrombus part was assigned a Young's modulus of 50,000 MPa and a Poisson's ratio of 0.48.[16,17] We used a 2:1 ratio and verified that the 2:1 ratio and the 20:1 ratios gave the same location of the peak wall stress.

The same boundary conditions were assigned to the 10 cases (5 patients, pre- and rupture analyses). A uniform blood pressure was applied onto the luminal surface (120 mmHg). The AAA was fixed at the renal arteries and the aortic bifurcation. It was assumed that there was no contact with neighbouring organs.

After performing the stress analysis, the following criteria were recorded: the mean of Peak Wall Stress (PWS), the 99th percentile of the PWS. The considered stress component was the first principal component. We used pre-rupture CT geometries to derive the peak wall stress and only used the post-rupture CT scan to compare rupture locations and peak stress locations.

Statistical Analysis

We conducted an observational analysis. Quantitative data were expressed as median (minimum-maximum) and qualitative data were expressed as numbers (percentage).

RESULTS

We retrospectively identified 5 patients corresponding to our inclusion criteria (Fig. 2). One patient came from the University hospital of Nancy, 1 patient came from the University hospital of Besancon and 3 patients came from the University hospital of Dijon. We included 5 patients, all men, who had a median age of 72 years (61–79). There was no history of diabetes, renal impairment or stroke. Four patients presented hypertension, 5 were smokers, 2 with dyslipidemia, coronary artery disease and peripheral arterial occlusive disease.

FEA were performed on 5 asymptomatic AAA, which ruptured secondarily. The median time

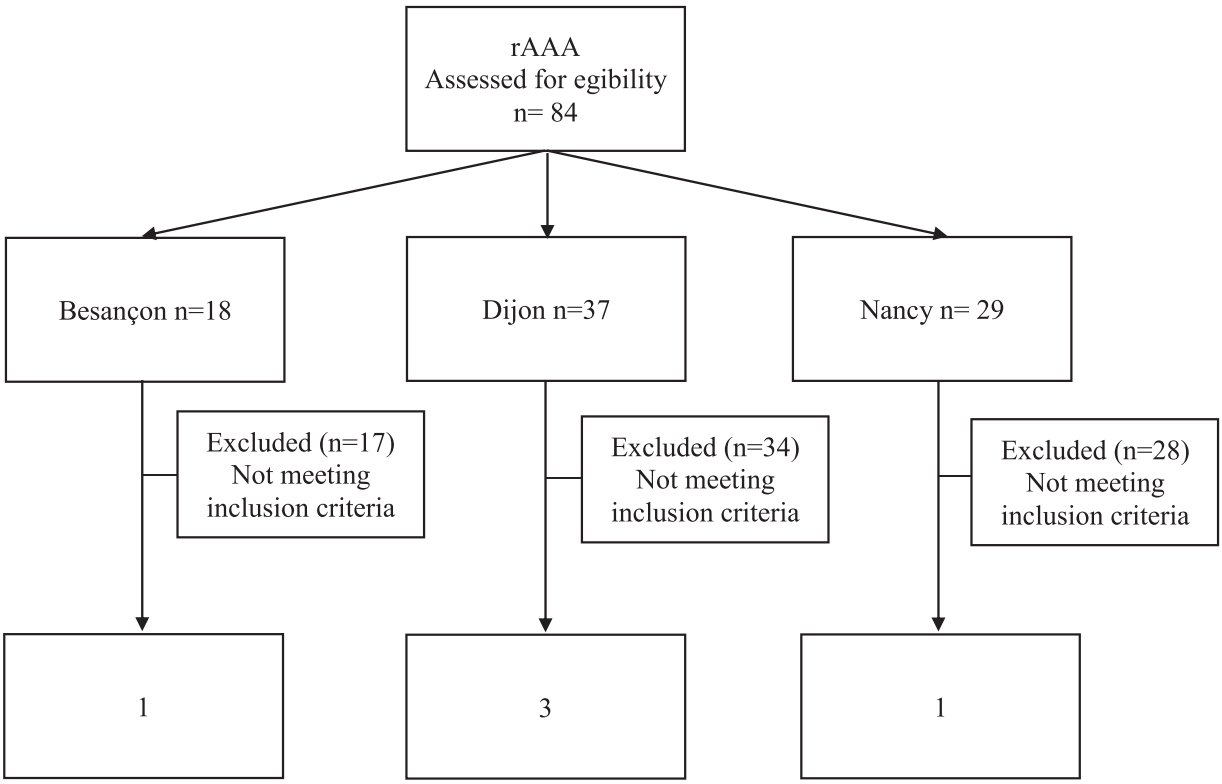

Fig. 2. Flow chart.

between the pre-rupture and rupture CT scans was 44 days (22–97). The AAA of Patient 1 had the characteristic of not presenting an intra-luminal thrombus (ILT).

Table I shows FEA calculated parameters. Pre-rupture and rupture FEAs were compared with the "thrombus" model and with the "wall" model. Respectively, the median was 0.365 MPa (0.291–0.753) and 0.390 MPa (0.343–0.819) for the "thrombus" model. The median was 0.817 MPa (0.555–1.295) and 1.160 MPa (0.633–1.625) for the "wall" model. The stresses observed on the "thrombus model" were higher in rupture than in pre-rupture stage, from 2.4 to 96.7%, without any link to the delay between the two CT scans. This was also observed in the "wall" model, from 8.8 to 98.9%, with the exception of 1 patient. In this "wall" model, the stresses were reduced by 10% for patient 4 in comparison with rupture. The stresses were marginally higher in the wall model compared to the thrombus model, from 83 to 254% range for the pre-rupture stage to 85–270% for the rupture stage. The rupture occurred for different inhomogeneous stress values. It was not possible to define a common stress threshold value for each AAA. Concerning the stress distribution, it seemed more obvious to find agreements in the wall model compared to the thrombus model (Figs. 3 and 4).

The site of rupture was not visible for patient 4. For other patients, the rupture site was visualized by contrast extravasation, wall continuity solution or intra-thrombus haemorrhage. There was an agreement between PWS and rupture site for a single patient (patient 1), the one who had the particularity of not presenting ILT (Table I) (Figure 5).

DISCUSSION

Rupture Threshold

FEA can predict the rupture risk of an AAA for a predefined blood pressure.[18] Through this work, we wanted to study more precisely the evolution of the peak wall stress based on pre-ruptured and ruptured scanographic data of AAA within a short period of 6 months preceding the rupture. There are only 2 other studies comparing pre-rupture and rupture CT scans of the same patients, but the time between aneurysm rupture and the pre-rupture scan was significantly larger: 308 days for the work of Erhart et al.[14] and 731 days for the work of Jalalzadeh et al.[19]

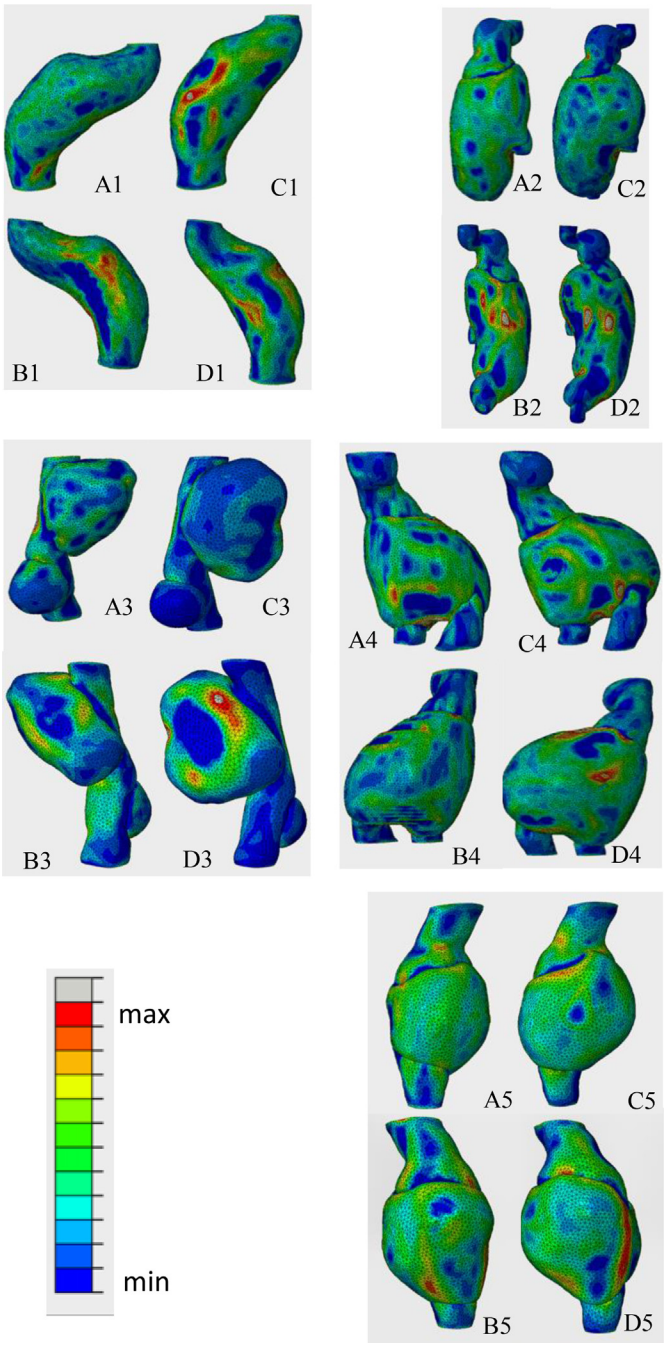

Fig. 3. Stress maps (first principal component) obtained with the FEA of the wall model. (Patient 1) A1: pre-rupture, anterior view (min +0.062 [MPa]; max +0.752 [MPa]). B1: pre-rupture, posterior view (min +0.062 [MPa]; max +0.752 [MPa]). C1: rupture, anterior view (min +0.068 [MPa]; max +0.819 [MPa]). D1: rupture, posterior view (min +0.068 [MPa]; max +0.819 [MPa]). (Patient 2) A2: pre-rupture, anterior view (min +0.079 [MPa]; max +0.959 [MPa]). B2: pre-rupture, posterior view (min +0.079 [MPa]; max +0.959 [MPa]). C2: rupture, anterior view (min +0.117 [MPa]; max +1.404 [MPa]). D2: rupture, posterior view (min +0.117 [MPa]; max +1.404 [MPa]). (Patient 3) A3: pre-rupture, anterior view (min +0.068 [MPa]; max +0.817 [MPa]). B3: pre-rupture wall model, posterior view (min +0.068 [MPa]; max +0.817 [MPa]). C3: rupture wall model, anterior view (min +0.135 [MPa]; max +1.625 [MPa]). D3: rupture wall model, posterior view (min +0.135 [MPa]; max +1.625 [MPa]). (Patient 4) A4: pre-rupture, anterior view (min +0.107 [MPa]; max +1.295 [MPa]). B4: pre-rupture, posterior view (min +0.107 [MPa]; max +1.295 [MPa]). C4: rupture, anterior view (min +0.096 [MPa]; max +1.160 [MPa]). D4: rupture, posterior view (min +0.096 [MPa]; max +1.160 [MPa]). (Patient 5) A5: pre-rupture, anterior view (min +0.046 [MPa]; max +0.554 [MPa]). B5: pre-rupture, posterior view (min +0.046 [MPa]; max +0.554 [MPa]). C5: rupture, anterior view (min +0.052 [MPa]; max +0.633 [MPa]). D5: rupture, posterior view (min +0.052 [MPa]; max +0.633 [MPa]).

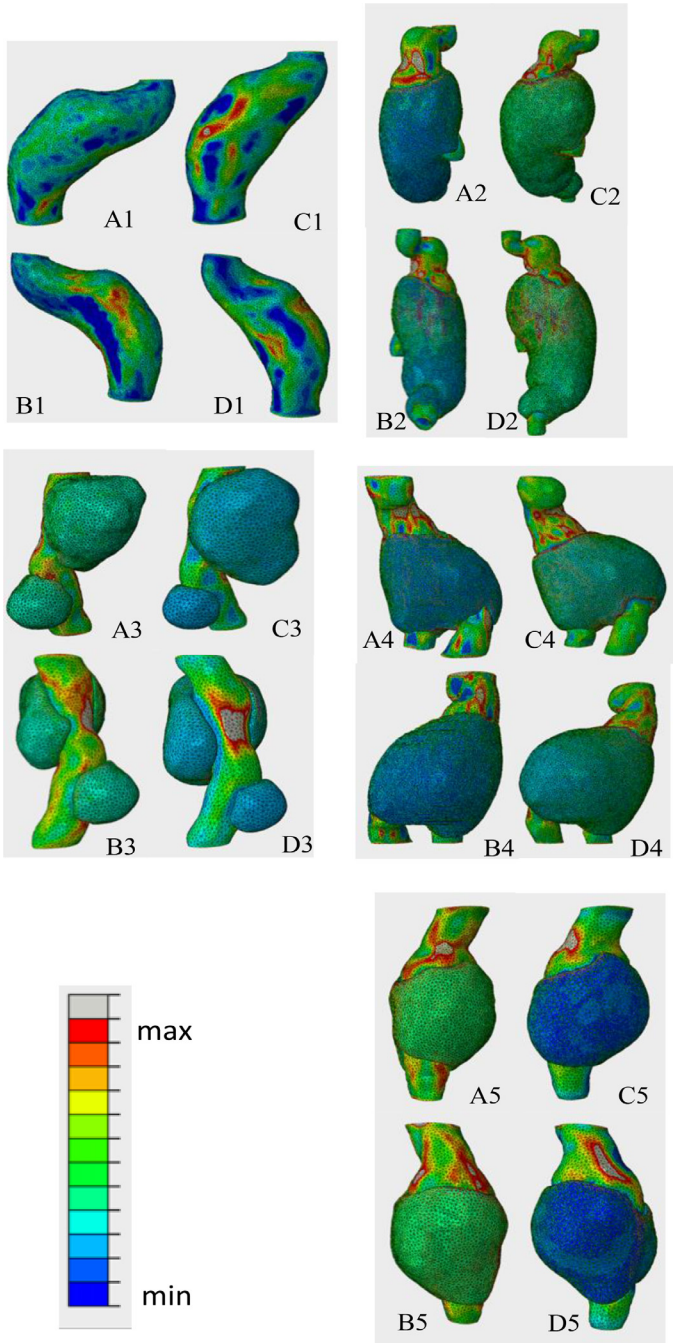

Fig. 4. Stress maps (first principal component, inner side of the wall) obtained with the FEA of the thrombus model. (Patient 1) A1: pre-rupture, anterior view (min +0.062 [MPa]; max +0.752 [MPa]). B1: pre-rupture, posterior view (min +0.062 [MPa]; max +0.752 [MPa]). C1: rupture, anterior view (min +0.068 [MPa]; max +0.819 [MPa]). D1: rupture, posterior view (min +0.068 [MPa]; max +0.819 [MPa]). (Patient 2) A2: pre-rupture, anterior view (min -0.070 [MPa]; max +0.370 [MPa]). B2: pre-rupture, posterior view (min -0.070 [MPa]; max +0.370 [MPa]). C2: rupture, anterior view (min -0.172 [MPa]; max +0.379 [MPa]). D2: rupture, posterior view (min -0.172 [MPa]; max +0.379 [MPa]). (Patient 3) A3: pre-rupture, anterior view (min -0.145 [MPa]; max +0.290 [MPa]). B3: pre-rupture, posterior view (min -0.145 [MPa]; max +0.290 [MPa]). C3: rupture, anterior view (min -0.143 [MPa]; max +0.572 [MPa]). D3: rupture, posterior view (min -0.143 [MPa]; max +0.572 [MPa]). (Patient 4) A4: pre-rupture, anterior view (min -0.044 [MPa]; max +0.365 [MPa]). B4: pre-rupture, posterior view (min -0.044 [MPa]; max +0.365 [MPa]). C4: rupture, anterior view (min -0.111 [MPa]; max +0.389 [MPa]). D4: rupture, posterior view (min -0.111 [MPa]; max +0.389 [MPa]). (Patient 5) A5: pre-rupture, anterior view (min -0.171 [MPa]; max +0.302 [MPa]). B5: pre-rupture, posterior view (min -0.171 [MPa]; max +0.302 [MPa]). C5: rupture, anterior view (min -0.031 [MPa]; max +0.343 [MPa]). D5: rupture, posterior view (min -0.031 [MPa]; max +0.343 [MPa]).

Please cite this article as: Lorandon *et al.*, Annals of Vascular Surgery(2021), https://doi.org/10.1016/j.avsg.2021.08.008

Table I. Morphological data and FEA calculated parameters of AAA

Patient	CT scan data					Thrombus model		Wall model	
		MAD (mm)				99th percentile stress (MPa)			
	Time between the two CT scan (days)	AAA pre ruptured	AAA ruptured	CTA rupture location	PWS location	AAA pre ruptured	AAA ruptured	AAA pre ruptured	AAA ruptured
1	97	54	59	Right anterior	Right anterior	0.753	0.819	0.753	0.819
2	44	74	76	Left lateral	Third proximal	0.370	0.379	0.959	1.404
3	22	51	57	Left postero-lateral	Right lateral	0.291	0.572	0.817	1.625
4	36	90	97	-	Third proximal	0.365	0.390	1.295	1.160
5	90	53	58	Left postero lateral	Right and left antero lateral	0.303	0.343	0.555	0.633

As expected, the stresses values of the rupture stage were larger than the pre-rupture stage. These results were consistent with the work of Erhart et al.[20]

The results of the study show a great dispersion of the stress values at rupture as well as a variability of the evolution during the last 6 months preceding the rupture. The rupture occurred for different stress values, with variations ranging from single to double. The rupture stress value seems intrinsically patient specific. This could easily be explained by the fact that strength values may vary significantly with the thrombus geometry, which was shown to play a prominent role on the proteolytic activity of the wall.[6,21,22] The study of the stress distribution of an AAA represents an indirect sign of rupture risk. This study does not allow to estimate the individual risk of rupture. The wall strength has to be determined in order to derive an individual risk. It should be highlighted that the largest stresses were predicted in the absence of thrombus. This could indicate a shielding role of the thrombus.[23] This would also confirm the role of the thrombus in causing indirectly a decrease of the wall strength due to the increased proteolytic activity. Accordingly, the wall model, though imperfect, can provide fast predictions. Published models over the last 10 years have attempted to approach reality, but there is still a pressing need of simple models that can estimate accurately AAA rupture risk.[24,25]

From the clinical point, these results have finally highlighted the need for ruptured or symptomatic AAA hospitalized patients to maintain minimal systolic blood pressure under 70–90 mmHg in order to decrease the stresses applied to the arterial wall.[26,27] Controlling the blood pressure would give important indications about the risk of rupture.

Correlation Between Rupture Site and Maximum Stress

We were able to find an agreement between the maximum stress location and the rupture site for only 1 out of the 5 patients, the 1 without thrombus. For the other patients, none of the models with or without ILT showed any correlation between the distribution of the maximum stress and the rupture site. Some studies on small cohorts have studied the correlation between PWS and rupture site. The results were contradictory. Some studies found a correlation between the rupture site and PWS or PWRR (PWS/Wall strength) location.[8,14,28] The fact that the PWS location and the rupture site agreed only for the thrombus-free patient could indicate that the thrombus would participate in a

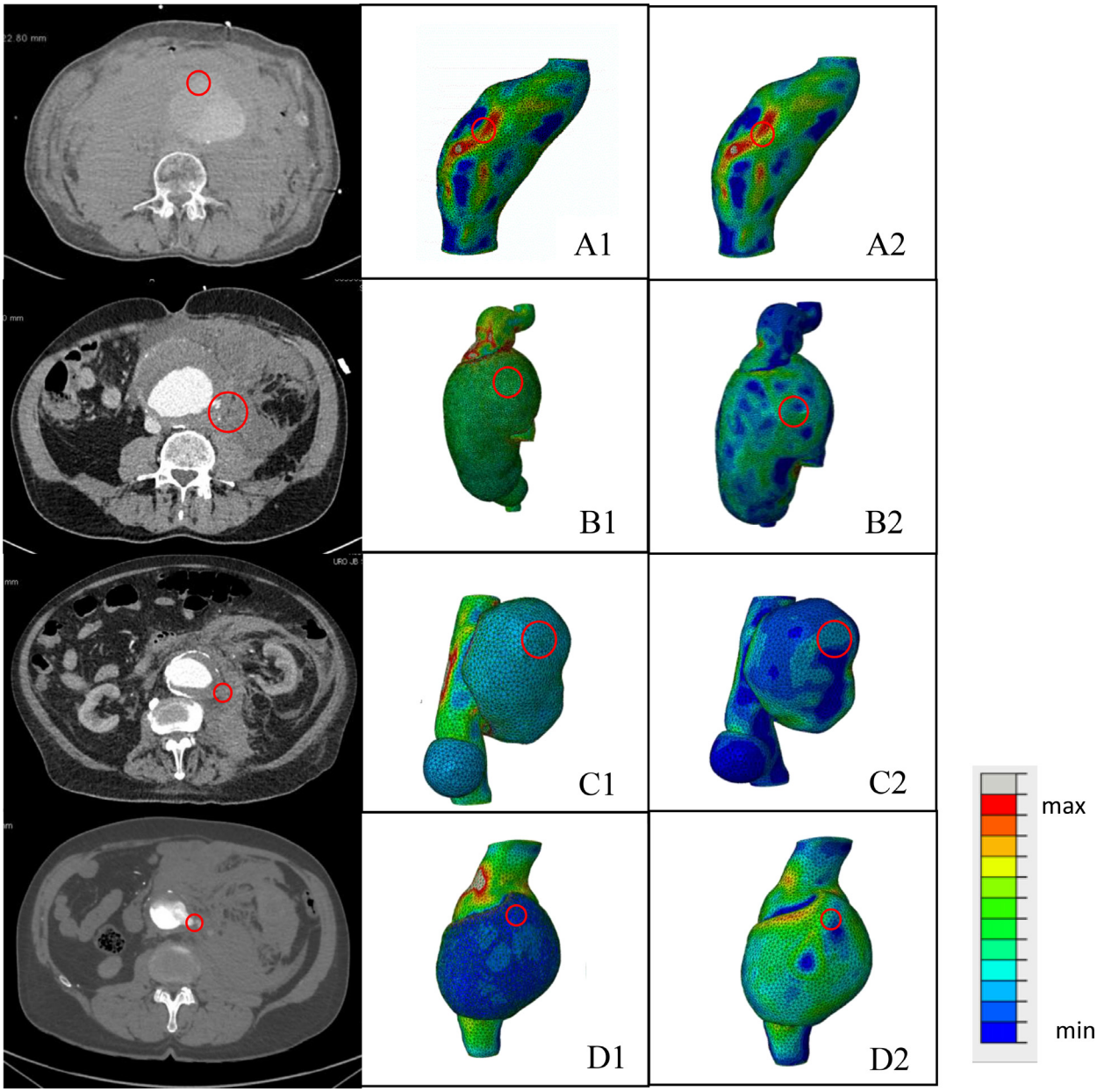

Fig. 5. CT scan and stress maps (first principal component) obtained with the FEA of ruptured AAA. The rupture site is visualized by the red circle; Patient 1: A1, rupture anterior view of the thrombus model (min +0.068 [MPa]; max +0.819 [MPa]); A2, rupture anterior view of the wall model (min +0.068 [MPa]; max +0.819 [MPa]). Patient 2: B1, rupture anterior view of thrombus model (min -0.172 [MPa]; max +0.379 [MPa]); B2, rupture anterior view of the wall model (min +0.117 [MPa]; max +1.404 [MPa]). Patient 3: C1, rupture anterior view of the thrombus model (min -0.143 [MPa]; max +0.572 [MPa]); C2, rupture anterior view of the wall model (min +0.135 [MPa]; max +1.625 [MPa]). Patient 5: D1, rupture anterior view of the thrombus model (min -0.031 [MPa]; max +0.343 [MPa]); D2, rupture anterior view of the wall model (min +0.052[MPa]; max +0.633[MPa]).

redistribution of the stresses applied to the wall, or that the thrombus would induce a local decrease of the wall strength due to larger proteolytic activity. Thus, the ILT could cause a change in the stresses applied to the aneurysmal wall and simultaneously a change of strength, related to its thickness and distribution. Doyle et al. studied CT data of a secondarily ruptured case. They observed that, on the pre-rupture data, the peak wall stress was located on the rupture site. However, only one case was presented in their study, which was an AAA without thrombus.[29]

Metaxa et al.[30] studied the failure site of an AAA. They were able to point out that the maximum stresses were located at the shoulders of the AAA and that the rupture occurred preferentially in the zone where the growth of the aneurysm was the most important. They also determined that the wall failure site did not coincide with the thrombus failure site. Thus, we could suggest that the maximum stresses were not a sufficient indicator for estimating the individual rupture risk. It appears that the patient-specific strength of the aneurysmal wall is needed to evaluate the rupture site, even when we have recent pre-rupture scans. Moreover, the thrombus plays an essential role on the stress distribution in the wall. The work of Wang et al.[31] also showed that the thrombus thickness would influence the localization of the maximum stress and the stress distribution. In addition, the rupture location in the thrombus does not correspond exactly to the rupture location in the wall as demonstrated by Metaxa et al., which emphasizes the complexity of the role played by ILT.[30]

It was observed that rupture occurs preferentially in the posterolateral region, which is in agreement with our results (3 patients out of 4). This observation could be related to the external constraints applied onto the AAA.[4] Moreover, the effects of surrounding tissues, not accounted for in our model, could explain the deviation between the actual rupture location and the location of peak wall stress. Farsad et al.[13] investigated the role of the spine in the development of AAA, showing that it could promote anterior and posterolateral AAA progression. Therefore, the spine therefore has an impact on the distribution of stresses on the wall. This is in agreement with the work of Kim et al.[32] on thoracic aortic aneurysms. They showed that the tissues surrounding the thoracic aorta should be taken into account when studying the stresses applied to the wall. Finally, studies on cerebral aneurysms have also highlighted the importance of the perianeurysmal tissue on rupture.[33]

As we applied a similar wall strength for all situations, we chose not to calculate the RPI.[34] Indeed, the RPI map would be similar to the stress map and the location of the peak wall stress would be the same as the location of peak RPI. A possible interesting future work would be to have regionally varying strength values to derive the RPI. However, assessing patient-specific and region-specific strength remains challenging.[35] These variabilities are the main reason explaining the discrepancy between the location of peak wall stress and the location of observed rupture.

Limitations of the Model

The small sample size is a limitation of this work. We favored short times between the two scans over the sample size, unlike other studies where the time between aneurysm rupture and the pre-rupture scans was significantly larger.[14,19]

Material properties cannot be derived from CT scans so the same model was used for all patients. The model did not take into account wall calcifications, surrounding organs, wall thickness and layer-specific material properties. To overcome these limitations, we used the Joldes approach,[16] which did not require information on material properties and neglects geometric nonlinearities.[10,17,36,37]

ILT modeling does not take into account all the complexity of its composition and its role in AAA rupture. The complexity of ILT mechanics deserves future studies to evaluate how it affects the location of the peak wall stress in the wall.[38]

We decided to use the 99th percentile stress which was more reliable as a biomechanical imaging marker than PWS, in order to avoid all false positives related to segmentation defects.[39,40]

We assumed a uniform 1.5 mm wall thickness as it was not possible to measure the thickness from CT scan data. However, adopting a constant wall thickness is one of the limitations of this work. Several studies[41–44] took into account the thickness of the wall to compute the wall stress in AAA. They observed that this had an impact on the distribution of stresses. Taking into account wall thickness could help to refine rupture site.

The remodeling related to the retro or intra-peritoneal hematoma complicated semi-automatic segmentation.

Due to lack of information, we had to apply a uniform blood pressure of 120 mmHg on all models. However, the occurrence of an AAA rupture leads to a state of hemorrhagic shock and therefore a modification of the stresses applied to the aneurysm wall.

Predictive Biomechanical Markers of Rupture

While many studies have highlighted the superiority of biomechanical markers,[10] the exact mechanism of AAA rupture is not yet known. It would seem that estimating such markers could be considered as indirect signs of increased risk of rupture. They could not be interpreted on an individual scale of risk of rupture.

To know to what stress the aneurysmal wall ruptures, it might be interesting to take into account

the stress values for a nonaneurysmal wall portion of the same patient or to try to determine the site of the wall with the lowest strength.

CONCLUSION

In conclusion, rupture risk estimation for AAA based on PWS presented a large inter-individual variability and did not correlate with the rupture site. We submitted that the site of rupture was determined by the regional variations of the wall resistance rather than the wall maximum stress and that the ILT played a major role in these variations.

ACKNOWLEDGMENTS

SA is grateful to the ERC through ERC-2014-CoG BIOLOCHANICS grant. We did not ask for ethics committees as we were outside the Jardé law. There was no change in current clinical practice.

REFERENCES

1. Brewster DC, Cronenwett JL, Hallett JW, et al. Guidelines for the treatment of abdominal aortic aneurysms. Report of a subcommittee of the Joint Council of the American Association for Vascular Surgery and Society for Vascular Surgery. J Vasc Surg 2003;37:1106–17.
2. Moll FL, Powell JT, Fraedrich G, et al. Management of abdominal aortic aneurysms clinical practice guidelines of the european society for vascular surgery. Eur J Vasc Endovasc Surg 2011;41:S1–58.
3. Chaikof EL, Dalman RL, Eskandari MK, et al. The Society for Vascular Surgery practice guidelines on the care of patients with an abdominal aortic aneurysm. J Vasc Surg 2018;67:2–77.e2.
4. Darling RC, Messina CR, Brewster DC, et al. Autopsy study of unoperated abdominal aortic aneurysms. The case for early resection. Circulation 1977;56(3):II161–4 Suppl.
5. Maier A, Gee MW, Reeps C, et al. A comparison of diameter, wall stress, and rupture potential index for abdominal aortic aneurysm rupture risk prediction. Ann Biomed Eng 2010;38:3124–34.
6. Gasser TC. Biomechanical rupture risk assessment: a consistent and objective decision-making tool for abdominal aortic aneurysm patients. Aorta Stamford Conn 2016;4:42–60.
7. Vande Geest JP, Di Martino ES, Bohra A, et al. A biomechanics-based rupture potential index for abdominal aortic aneurysm risk assessment: demonstrative application. Ann N Y Acad Sci 2006;1085:11–21.
8. Doyle BJ, Coyle P, Kavanagh EG, et al. A Finite Element Analysis Rupture Index (FEARI) Assessment of Electively Repaired and Symptomatic/Ruptured Abdominal Aortic Aneurysms. In: 6th World Congress of Biomechanics (WCB 2010). Singapore: Springer, Berlin, Heidelberg; August 1-6, 2010. p. 883–6. 2010.
9. Leemans EL, Willems TP, van der Laan MJ, et al. Biomechanical indices for rupture risk estimation in abdominal aortic aneurysms. J Endovasc Ther 2017;24:254–61.
10. Farotto D, Segers P, Meuris B, et al. The role of biomechanics in aortic aneurysm management: requirements, open problems and future prospects. J Mech Behav Biomed Mater 2018;77:295–307.
11. Wadgaonkar AD, Black JH, Weihe EK, et al. Abdominal aortic aneurysms revisited: MDCT with multiplanar reconstructions for identifying indicators of instability in the pre- and postoperative patient. Radiographics 2015;35:254–68.
12. Walker ST, Pipinos II, Johanning JM, et al. Contained rupture of an abdominal aortic aneurysm with extensive vertebral body and retroperitoneal space destruction. J Comput Assist Tomogr 2017;41:839–42.
13 Farsad M, Zeinali-Davarani S, Choi J, et al. Computational growth and remodeling of abdominal aortic aneurysms constrained by the spine. J Biomech Eng 2015;137:0910081–09100812. doi:10.1115/1.4031019.
14. Erhart P, Roy J, de Vries J-PPM, et al. Prediction of rupture sites in abdominal aortic aneurysms after finite element analysis. J Endovasc Ther 2016;23:115–20.
15. Raut SS, Chandra S, Shum J, et al. The role of geometric and biomechanical factors in abdominal aortic aneurysm rupture risk assessment. Ann Biomed Eng 2013;41:1459–77.
16. Joldes GR, Miller K, Wittek A, et al. A simple, effective and clinically applicable method to compute abdominal aortic aneurysm wall stress. J Mech Behav Biomed Mater 2016;58:139–48.
17. Joldes GR, Miller K, Wittek A, et al. BioPARR: a software system for estimating the rupture potential index for abdominal aortic aneurysms. Sci Rep 2017;7:4641.
18. Fillinger MF, Marra SP, Raghavan ML, et al. Prediction of rupture risk in abdominal aortic aneurysm during observation: wall stress versus diameter. J Vasc Surg 2003;37:724–32.
19. Jalalzadeh H, Leemans EL, Indrakusuma R, et al. Estimation of abdominal aortic aneurysm rupture risk with biomechanical imaging markers. J Vasc Interv Radiol 2019;30:987–994.e4.
20. Erhart P, Hyhlik-Dürr A, Geisbüsch P, et al. Finite element analysis in asymptomatic, symptomatic, and ruptured abdominal aortic aneurysms: in search of new rupture risk predictors. Eur J Vasc Endovasc Surg 2015;49:239–45.
21. Stevens RRF, Grytsan A, Biasetti J, et al. Biomechanical changes during abdominal aortic aneurysm growth. PloS One 2017;12:e0187421.
22. Chauhan SS, Gutierrez CA, Thirugnanasambandam M, et al. The association between geometry and wall stress in emergently repaired abdominal aortic aneurysms. Ann Biomed Eng 2017;45:1908–16.
23 Kontopodis N, Koncar I, Tzirakis K, et al. Intraluminal thrombus deposition is reduced in ruptured compared to diameter matched intact abdominal aortic aneurysms. Ann Vasc Surg 2018;55:189–95 PMID: 30287289. doi:10.1016/j.avsg.2018.07.048.
24. Malkawi AH, Hinchliffe RJ, Xu Y, et al. Patient-specific biomechanical profiling in abdominal aortic aneurysm development and rupture. J Vasc Surg 2010;52:480–8.
25. Gasser TC, Auer M, Labruto F, et al. Biomechanical rupture risk assessment of abdominal aortic aneurysms: model complexity versus predictability of finite element

simulations. Eur J Vasc Endovasc Surg 2010;40:176–185.
26. Reimerink JJ, van der Laan MJ, Koelemay MJ, et al. Systematic review and meta-analysis of population-based mortality from ruptured abdominal aortic aneurysm. Br J Surg 2013;100:1405–13.
27. Ohki T, Veith FJ. Endovascular grafts and other image-guided catheter-based adjuncts to improve the treatment of ruptured aortoiliac aneurysms. Ann Surg 2000;232:466–479.
28. Venkatasubramaniam AK, Fagan MJ, Mehta T, et al. A comparative study of aortic wall stress using finite element analysis for ruptured and non-ruptured abdominal aortic aneurysms. Eur J Vasc Endovasc Surg 2004;28:168–76.
29. Doyle BJ, McGloughlin TM, Miller K, et al. Regions of high wall stress can predict the future location of rupture of abdominal aortic aneurysm. Cardiovasc Intervent Radiol 2014;37:815–18.
30. Metaxa E, Tzirakis K, Kontopodis N, et al. Correlation of intraluminal thrombus deposition, biomechanics, and hemodynamics with surface growth and rupture in abdominal aortic aneurysm-application in a clinical paradigm. Ann Vasc Surg 2018;46:357–66.
31. Wang DHJ, Makaroun MS, Webster MW, et al. Effect of intraluminal thrombus on wall stress in patient-specific models of abdominal aortic aneurysm. J Vasc Surg 2002;36:598–604.
32. Kim J, Peruski B, Hunley C, et al. Influence of surrounding tissues on biomechanics of aortic wall. Int J Exp Comput Biomech 2013;2:105–17.
33. Sugiu K, Jean B, San Millan Ruiz D, et al. Influence of the perianeurysmal environment on rupture of cerebral aneurysms. Preliminary observation. Interv Neuroradiol J 2000;6(1):65–70 Suppl.
34. Vande Geest JP, Di Martino ES, Bohra A, et al. A biomechanics-based rupture potential index for abdominal aortic aneurysm risk assessment: demonstrative application. Ann N Y Acad Sci 2006;1085:11–21.
35. Azar D, Ohadi D, Rachev A, et al. Mechanical and geometrical determinants of wall stress in abdominal aortic aneurysms: a computational study. PloS One 2018;13 e0192032.
36 Novak K, Polzer S, Bursa J. Applicability of simplified computational models in prediction of peak wall stress in abdominal aortic aneurysms. Technol Health Care 2017;26(1):165–73 PMID: 29172016. doi:10.3233/THC-171024.
37. Kontopodis N, Metaxa E, Papaharilaou Y, et al. Advancements in identifying biomechanical determinants for abdominal aortic aneurysm rupture. Vascular 2015;23:65–77.
38. O'Leary SA, Kavanagh EG, Grace PA, et al. The biaxial mechanical behaviour of abdominal aortic aneurysm intraluminal thrombus: classification of morphology and the determination of layer and region specific properties. J Biomech 2014;47:1430–7.
39. Indrakusuma R, Jalalzadeh H, Planken RN, et al. Biomechanical imaging markers as predictors of abdominal aortic aneurysm growth or rupture: a systematic review. Eur J Vasc Endovasc Surg 2016;52:475–86.
40. Speelman L, Bosboom EMH, Schurink GWH, et al. Patient-specific AAA wall stress analysis: 99-percentile versus peak stress. Eur J Vasc Endovasc Surg 2008;36:668–76.
41. Raut SS, Liu P, Finol EA. An approach for patient-specific multi-domain vascular mesh generation featuring spatially varying wall thickness modeling. J Biomech 2015;48:1972–81.
42. Shang EK, Nathan DP, Woo EY, et al. Local wall thickness in finite element models improves prediction of abdominal aortic aneurysm growth. J Vasc Surg 2015;61:217–23.
43. Conlisk N, Geers AJ, McBride OMB, et al. Patient-specific modelling of abdominal aortic aneurysms: The influence of wall thickness on predicted clinical outcomes. Med Eng Phys 2016;38:526–37.
44 Biehler J, Wall WA. The impact of personalized probabilistic wall thickness models on peak wall stress in abdominal aortic aneurysms. Int J Numer Methods Biomed Eng 2018;34(e2922).